ELSEVIER

Biophysical Chemistry 75 (1998) 45–55

Biophysical Chemistry

Plant sterols: a neutron diffraction study of sitosterol and stigmasterol in soybean phosphatidylcholine membranes

M.P. Marsan[1,a], E. Bellet-Amalric[1b], I. Muller[a], G. Zaccai[b,c], A. Milon[a,*]

[a] *Institut de Pharmacologie et de Biologie Structurale, CNRS, 205 Rte de Narbonne, 31077 Toulouse Cédex, France*
[b] *Institut Laue Langevin, Avenue des Martyrs, B.P. 156X, 38042 Grenoble Cedex, France*
[c] *Institut de Biologie Structurale, CEA-CNRS, 41 Avenue des Martyrs, 38027 Grenoble Cedex, France*

Received 16 March 1998; received in revised form 10 July 1998; accepted 10 July 1998

Abstract

Neutron scattering experiments have been performed on oriented Soybean phosphatidylcholine (SPC) bilayers, containing sitosterol or stigmasterol, two major sterols of plant plasma membranes. Sitosterol and stigmasterol were either protonated or deuterated on position C_{25} of the lateral chain. Incorporation of sitosterol leads to an increase of the hydrophobic thickness of SPC bilayers of 1.2 and 2 Å when present, at 16 and 30 mol%, respectively. On the other hand, no change was observed when stigmasterol is present in the bilayer at its maximal solubility of 16 mol%. These results are in agreement with the fact that sitosterol is more efficient than stigmasterol to order acyl chains of SPC, as already shown with other biophysical techniques. In order to get more insight into the behavior of the lateral chains of the two sterols, the proton–deuterium contrast method was used in order to locate the $^2H_{25}$ atoms of the two sterols. For sitosterol, this atom was found close to the center of the bilayer at $\pm(1.6 \pm 0.2$ Å), with a width, $\nu = 2.5 \pm 0.5$ Å. For stigmasterol, the difference profile could be fitted in two different ways: either two possible locations are found at $\pm(2.3 \pm 0.2$ Å) and $\pm(10 \pm 0.2$ Å) with the same width, $\nu = 2.5 \pm 0.5$ Å or only one broad distribution at $\pm(6.1 \pm 0.3$ Å), $\nu = 8.5 \pm 0.7$ Å. The results are discussed in terms of difference of dynamics for the lateral chain of the two sterols.

Keywords: Bilayer thickness; Deuterium-labeled sterols; Oriented bilayers; Plant lipids; Side chain dynamics

* Corresponding author. Tel.: +33 561175423; e-mail: milon@ipbs.fr

Abbreviations: SPC, soybean phosphatidylcholine; DMPC, dimyristoylphosphatidylcholine; BHT, butylated hydroxytoluene

[1] These two authors contributed equally to the work.

0301-4622/98/$19.00
PII S0301-4622(98)00188-4

1. Introduction

Sterols play an important role as membrane components and are implicated in the regulation of properties such as permeability and fluidity [1,2]. Cholesterol is the major sterol in membranes of animal cells, while plant cells contain a complex mixture in which sitosterol, stigmasterol and 24-methyl-cholesterol often predominate. Deuterium nuclear magnetic resonance (^{2}H-NMR) studies, with deuterated phospholipids, have shown the influence of sterols on acyl chain order parameters [3,4]. ^{2}H-NMR and neutron diffraction experiments have led to the location of specifically deuterated cholesterol embedded in the lipid bilayer [1,5–7]. The ability of plant sterols to order fatty acyl chains of soybean phosphatidylcholine (SPC) was also investigated [8,9]. The most striking result of these studies was the good efficiency of cholesterol and sitosterol towards lipid ordering and the bad ordering ability of stigmasterol; sitosterol and stigmasterol (Fig. 1) differ only by a supplementary double bond on the side chain of stigmasterol. To get more insight into the molecular mechanisms of plant sterol–plant lipid interactions, we undertook a study of these interactions by deuterium NMR [10] and neutron diffraction.

The main advantage of neutron scattering derives from the large difference in the coherent scattering amplitudes of the hydrogen and deuterium nuclei. Contrary to X-rays, which interact with electrons, neutrons interact with atomic nuclei and distinguish between different isotopes. Neutrons are scattered by most components in living cells with negligible absorption. Neutron diffraction has been used to provide precise information on biological systems as for example on the structure and the extent of disorder in lipid membranes [11–15]. This technique combined with the use of specifically deuterated membrane components can provide the location of deuterium labels in the thickness of the membrane.

The studies reported here were performed in order to determine the location of the plant sterols, sitosterol and stigmasterol, within the lipid bilayer. More specifically, the aim was to provide a structural understanding of the different effects of the two major plant sterols.

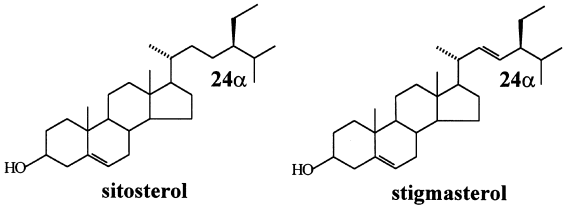

Fig. 1. Structure of sitosterol (a) and stigmasterol (b).

2. Experimental

2.1. Sample preparation

Samples of oriented lipid multilayers were prepared with SPC [25 mg, 73 mol% (Sigma)], DMPC [3 mg, 10 mol% (Sygena, Inc., Liestal)], BHT [1 mol% (Sigma)] and sterol (3 mg, 16 mol% or 6 mg, 30 mol%). The fatty acid composition of SPC was previously determined by gas chromatography of the corresponding methyl esters [16]. It consists of a majority of polyunsaturated C_{18} fatty acids: 13.5% of C16:0, 4% of C18:0, 12% of C18:1, 63% of C18:2, 6.5% of C18:3 and 1% of others. In each sample, 10 mol% DMPC was added in order to be consistent with previous work using deuterium NMR and sn2-deuterated DMPC (used as a molecular probe of the acyl chain order parameters) [8,9]. BHT was added at a final concentration of 1 mol% to avoid oxidation of polyunsaturated acyl chains. The 25-labeled sitosterol and stigmasterol were synthesized in our group [10]. The lipid mixture was dissolved in isopropanol and deposited onto a microscope slide (28×36 mm) previously treated by 12-h immersion in fuming nitric acid. The plates were placed under vacuum for 12 h to remove the solvent and then hydrated for 12 h at room temperature in the presence of saturated KCl (85% relative humidity). Three hydration–dehydration cycles were applied to each sample; the dehydration was performed under high vacuum during 12 h. This procedure, used to ensure good orientation, was repeated for samples containing the non-deuterated sterols, sitosterol and stigmasterol and those with the two deuterated

sterols. Samples were hydrated with different ^2H_2O contents: 0, 50 and 100% (KCl saturated). A list of the samples and abbreviations used is reported in Table 1. Samples of same lipid compositions (including 1 mol% of BHT, which is known to protect unsaturated lipids from oxidation) but containing 10 mol% of perdeuterated sn-2 acyl chain DMPC instead of non-labeled DMPC were treated in the same conditions than the samples used herein. ^{2}H-NMR spectra were recorded after three dehydration–hydration cycles and 10 and 20 h later. No modification of the spectra were observed over time indicating that the samples were not altered.

2.2. Neutron diffraction

2.2.1. Data collection

Diffraction experiments on the oriented lipid samples were performed on the D16 neutron diffractometer at the Institut Laue Langevin (Grenoble, France). Cold neutrons of wavelength 4.52 Å were selected by a pyrolitic graphite monochromator and detected by a bidimensional ^{3}He neutron counter of 64 horizontal wires covering a 9° angle 1 m from the sample and 16 wires covering a 4.5 Å angle in the vertical direction. A low efficiency detector (the monitor) monitored the incident neutron beam.

The sample slides were mounted on a goniometer placed in a closed aluminium can in the presence of saturated KCl. Temperature control was achieved by circulating water in the can wall from a thermostated bath at 20°C. The sample was equilibrated for at least 10 h before diffraction was measured.

The diffracted reflections were measured, with the detector center placed at $2\theta_B$, θ_B being the Bragg angle, by scanning the sample over $\pm 0.5°$ around θ_B. For each sample, data were recorded for two or three cycles to check for reproducibility of the measurements.

The mosaic spread of each sample was also measured on the second diffraction order by scanning the sample while keeping the detector at a constant angle. The mosaicity, ranging from 2 to 5°, corresponds to a fairly good orientation.

2.2.2. Data reduction

A first integration was achieved by adding the intensity vertically, wire-by-wire. The detector efficiency was calibrated by using the scattering of H_2O in a 1-mm thick quartz cell, which is essentially incoherent and constant in the angular range measured. The total intensity for each order, h, $I(h)$, was obtained by integration of the Bragg peaks along the 2θ-axis over 1.5° with linear background subtraction. Data were normalized to a constant monitor count.

The absolute values of the structure factors $F(h)$ were calculated from the measured intensities by the following relation [11]:

$$|F(h)| = \left(\frac{I(h)R(h)}{a(h)L(h)} \right)^{1/2} \quad (1)$$

where $R(h)$ is the geometric factor due to the limited vertical acceptance of the detector, $a(h)$ is the absorption correction and $L(h)$ is the Lorentz factor.

The absorption coefficients $a(h)$, include the true absorption (negligible) and the incoherent scattering of the incident beam by the sample. For a one-dimensional crystal, such as bilayers on

Table 1
Samples used in this work

Sample description	Abbreviations
SPC/DMPC 10 mol%	spc
SPC/DMPC 10 mol%/sitosterol 16 mol%	sito16
SPC/DMPC 10 mol%/[25-^{2}H]sitosterol 16 mol%	sitod16
SPC/DMPC 10 mol%/[25-^{2}H]sitosterol 30 mol%	sitod30
SPC/DMPC 10 mol%/stigmasterol 16 mol%	stigma16
SPC/DMPC 10 mol%/[25-^{2}H]stigmasterol 16 mol%	stigmad16

a plate, $a(h)$ is characteristic of the considered sample and is calculated for each order [12]:

$$a(h) = \frac{\lambda h}{4\mu t}\left(1 - \exp\left(\frac{-4\mu dt}{\lambda h}\right)\right) \quad (2)$$

where λ is the wavelength (4.52 Å), μ the attenuation factor [μ (cm^{-1}) = 6.04–0.75 χ_{D_2O}), χ_{D_2O} being the fraction of deuterated water [5], d the lamellar spacing and t the thickness of the sample (between 35 and 40 μm for the lipid mixture studied). The lamellar spacing was obtained by fitting the peak positions according to Bragg's law: $2d \sin \theta_B(h) = h\lambda$.

The Lorentz factor, in the case of oriented bilayers, is $1/\sin 2\theta_B$ [17].

The vertical extension of the Bragg peaks results from the convolution of the sample mosaicity with the beam geometry. Corrections for vertical smearing were applied (Gordeliy et al., to be published). For our samples $R(h)$ was less than 1.1.

2.2.3. Phasing of structure factors

For centrosymmetric unit cells, as is the case for our samples, the structure factors are real numbers and their phases are either 0 or π. Since the Fourier transform of a hydrated structure depends linearly (for each order) on the ^2H_2O concentration, it is possible to determine the relative sign in H_2O and ^2H_2O [5]. Therefore the structure factors $F(h)$ were measured for three isotopic concentrations (0, 50 and 100% ^2H_2O).

For the H_2O profile the first two phases were fixed by placing the origin at the center of the bilayer and by selecting a positive scattering density difference between the headgroups and the bilayer center [15]. The third and fourth phases were chosen in order to produce a flat ^2H_2O–H_2O profile in the hydrophobic part of the bilayer ($\pm$10 Å). The phase of the fifth order was selected to get a typical bilayer profile with a marked minimum at the center [5].

Scattering profiles in real space $\rho(x)$ for each sample were derived from the Fourier transform of the structure factors:

$$\rho(x) = \frac{1}{d}F(0) + A\frac{2}{d}\sum_{h=1}^{h=5} F(h)\cos\left(\frac{2\pi hx}{d}\right) \quad (3)$$

where $F(0)$ is the zero order structure factor (equal to the scattering density of the unit cell), x is the distance from the bilayer center along the direction normal to the bilayer surface and A is a scaling factor which puts the profile on an absolute scale.

The values of $F(0)$ were calculated from neutron scattering length densities [5], partial volumes of sample components [18] and assuming 10 water molecules per lipid molecule [19,20] (see Table 2). Accurate water content measurements are not trivial to perform for lipid systems [20]. The figure of 10 water molecules was previously measured for PC head groups and various chain types (egg yolk PC and dioleylPC [20] and dipalmitoylPC [19]) in similar humidity conditions. In any case the calculation is insensitive to a variation of 20% in this number.

For the sterols the same density as cholesterol (1.03 g/cm^3) was used [21]. The scaling factor A was calculated assuming that there is a distinct water layer (whose scattering density is -0.0056×10^{-12} cm/Å^3) between the lipid bilayers. It was adjusted slightly for self-consistency between the deuterium-labeled and unlabeled samples.

For samples with a deuterium label (position 25 of each of the two plant sterols), the substitution was considered to be isomorphous. Indeed, the d spacing were found to be identical within experimental errors. The labeled position results from

Table 2
Neutron scattering amplitude densities and occupation volumes of H_2O, D_2O and the different chemical groups in the lipid bilayers

	Neutron scattering amplitude density (10^{-12} cm/Å^3)	Volume[a] (Å^3)
H_2O	−0.0056	30
D_2O	+0.0638	30
CH_2	−0.0031	27
CH_3	−0253.0085	54
Polar group[b]	+0.0167	360

[a] Tardieu and Luzzati [18].
[b] Glycero phosphorylcholine plus the carboxylic groups.

the difference between the labeled, $\rho_D(x)$, and the non-labeled, $\rho_H(x)$ profiles:

$$\rho_{label}(x) = \rho_D(x) - \rho_H(x) \quad (4)$$

The label distribution profile $\rho_{label}(x)$ was modeled as the sum of two Gaussian distributions centered on $\pm x_0$ and of equal width ν:

$$\rho_{label}(x) = \frac{n(b_D - b_H)}{\pi^{1/2}\nu S}\left\{\exp\left(\frac{-(x-x_0)}{\nu}\right)^2 + \exp\left(\frac{-(x+x_0)}{\nu}\right)^2\right\} \quad (5)$$

where n is the number of D atoms, b_D and b_H are the neutron scattering lengths of deuterium and hydrogen nuclei, S the area per lipid molecule in the bilayer surface. ν is related to the distribution width [$\nu = (FWHM)/(2\sqrt{\ln 2})$].

3. Results

Diffraction patterns were recorded for the six different samples of Table 1. The samples were identical to those used previously for ^{2}H-NMR studies in order to allow a direct comparison [8,9]. The maximal solubility of stigmasterol in SPC is 16 mol% compared to 30 mol% for sitosterol. The sample containing 16 mol% sitosterol was analyzed at three ^2H_2O concentrations, 0, 50 and 100%, in order to determine the signs of the structure factors.

For each lipid mixture, significant intensities were obtained only for the first five orders. Even with longer counting times (6 h/order), higher orders could not be observed. This probably reflects the higher mobility of polyunsaturated fatty acids and the fact that a complex mixture of lipids is used. Table 3 summarizes the diffracted intensities, $I(h)$, of the five orders for the sito16 sample in different water contrast. These intensities were measured over 24 h. Statistical errors are lower than 1% for large $I(h)$ values and can reach 3% for weak ones. The effects of systematic errors arising from background subtraction, vertical aperture, absorption correction, etc., were minimized by treating the data from all samples in an identical way.

Fig. 2 shows the linear dependence of $F(h)$ vs. ^2H_2O concentration for the five orders. $F(h)$ is of the same sign for the first and the fourth diffraction orders, and of opposite sign for the second and the third orders. In ^2H_2O the intensity of the first order increases strongly, and the measured value is lower than expected due to extinction [5]. From Fig. 2 it is clear that a linear dependence would increase $F(1)$ in ^2H_2O by 20%. For the water profiles calculation we used the corrected value. The signs of the structure factors for each order were chosen according to the procedure described in Section 2.2 (see Fig. 2).

The first four structure factors were phased by using the data obtained from 100% and 0% ^2H_2O on a Hargreave's plot as described by Zaccai et al. [22]. This approach is based on the isomor-

Table 3
Diffracted intensities and structure factors corresponding to the five orders of diffraction observed on the SPC/DMPC/sitosterol 16 mol% sample hydrated in H_2O–^2H_2O mixtures

Order	0% ^2H_2O		50% ^2H_2O		100% ^2H_2O	
	$I(h)$[a]	$F(h)$[b]	$I(h)$	$F(h)$	$I(h)$	$F(h)$
1	17460	−50.0	346.10^3	−221	875.10^3	−300
2	17590	−63.4	7810	+41.7	247.10^3	+116
3	10260	+57.0	900	+16.6	15280	−13.2
4	3930	−39.6	2090	−28.5	21110	−24.8
5	610	−17.1	360	−12.9	6310	−13.0
d-spacing	50.61 ± 0.08 Å		50.0 ± 0.2 Å		50.5 ± 0.4 Å	

[a]All the intensities are normalized to the same monitor.
[b]The structure factors were calculated using Eq. (1).

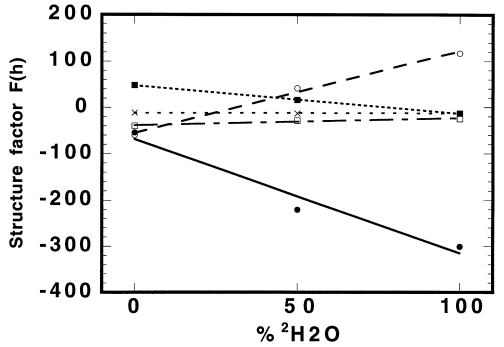

Fig. 2. Dependence of the structure factors $F(h)$ for the sitosterol 16 mol% sample on ^2H_2O concentration: ●, $F(1)$; ○, $F(2)$; ■, $F(3)$; □, $F(4)$; x, $F(5)$.

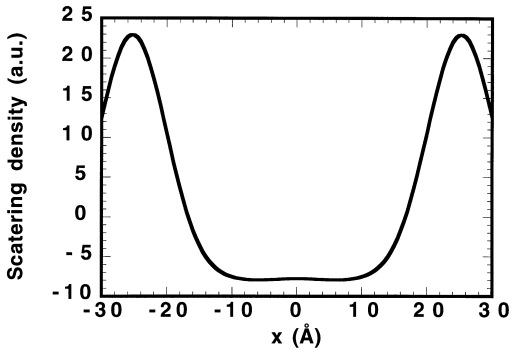

Fig. 3. Difference neutron density scattering profile showing the distribution of water in oriented bilayers of SPC/DMPC 10 mol%/sitosterol 16 mol%. The origin is at the bilayer center.

phous replacement of H_2O by ^2H_2O at $\pm d/2$. The resulting signs in H_2O are $(-,-,+,-)$, consistent with the literature [11,13,23,24]. The corresponding water profile is shown in Fig. 3. As expected from the phasing procedure the profile peaks in between the head groups and is flat at the bilayer center. The determination of the sign of the fifth order was not straightforward, as it varies with lipid composition and temperature [5,11,24–26], and the water profile is not sensitive to this phase, in our case. Our choice was based on the shape of the bilayer profile, with a real minimum at the center of the bilayer corresponding to the CH_3 groups. The phase sequence used in light water was then $(-,-,+,-,-)$. Moreover, only this set of phases gives a sterol influence compatible with the cholesterol effect [5,26] as will be seen below. For the other samples we assumed there was no change of phases.

3.1. The SPC, SITO16 and STIGMA16 samples

Fig. 4 represents the neutron scattering density profiles of the lipid bilayer for the SPC, sito16 and stigma16 samples. The scattering densities were calculated from the values of Table 4, using Eq. (3).

For the lipid membrane the positive peaks on either side of the hydrocarbon region, at approx. ± 16.5 Å from the center, correspond to the carbonyl groups and oxygen atoms of the ester linkage between the fatty acid and the glycerol, as confirmed by the scattering density of $0.0167 \times$

Table 4
Summary of data for the six samples analyzed

	$F(1)^a$	$F(2)^a$	$F(3)^a$	$F(4)^a$	$F(5)^a$	$F(0)/d^b$ (10^{-12} cm/Å^3)	A^c (10^{-12}cm/Å^3)	d (Å)^d	d_L (Å)^e
spc	−37	−46	41	−25	−12	0.00277	0.00170	49.51 ± 0.07	32.8
sito16	−54	−60	48	−39	−11	0.00295	0.00132	50.61 ± 0.08	34.0
sitod16	−48	−54	46	−35	−10	0.00315	0.00141	50.77 ± 0.08	34.2
sitod30	−40	−43	35	−29	−6	0.00350	0.00192	51.04 ± 0.06	34.8
stigma16	−49	−63	57	−39	−17	0.00297	0.00116	49.75 ± 0.05	33.0
stigma d16	−30	−48	42	−27	−11	0.00313	0.00143	49.90 ± 0.08	33.0

[a] Structure factors $F(h)$ calculated using Eq. (1).
[b] Zero order structure factor.
[c] Scaling factor by which the structure factor should be multiplied to have a density profile in absolute scale.
[d] Lattice spacing.
[e] d_L peak-to-peak distance, also called hydrophobic distance.

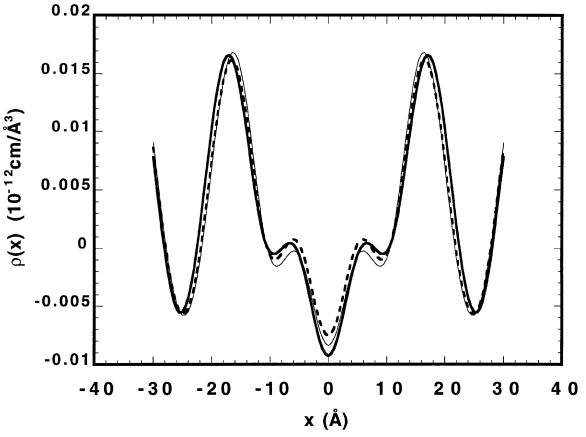

Fig. 4. Scattering profiles for the samples: SPC/DMPC 10 mol% (thin line); SPC/DMPC 10 mol%/sitosterol 16 mol% (thick line); SPC/DMPC 10 mol%/stigmasterol 16 mol% (dashed line).

10^{-12} cm/Å^3 (see Table 2). The hydrophobic distance d_L of 32.8 Å, corresponding to the distance between these two peaks is comparable to the 34 Å found for DOPC (two C18:1 chains) [25].

A clear negative minimum (-0.0082×10^{-12} cm/Å^3) at the center of the bilayer reflects the concentration of methyl groups. The oscillation at approx. ± 6–10 Å is due to series termination errors. The two extreme parts of the profile (density of -0.0056×10^{-12} cm/Å^3 at $-d/2$, $+d/2$) represent the water layer.

The addition of 16 mol% sitosterol or stigmasterol leads to a series of modifications as compared to the SPC sample (Fig. 4). The scattering density of the positive peaks at ± 18 Å decreases while the scattering profile at approx. ± 6–10 Å increases. The lattice spacing is slightly larger ($+0.2$ Å) for stigmasterol and significantly larger for sitosterol ($+1.2$ Å). At the center of the bilayer the scattering density is lower for sitosterol but higher for stigmasterol.

Inspection of the profiles suggests that the increase in periodicity is due to an increase of d_L at constant hydration. The absolute values of d_L may be affected by several parameters such as the number of measurable diffraction orders and correction factors used in the calculation of structure factors. Nevertheless, d_L values were reproducible to ± 0.1 Å for four independent measurements of the diffracted intensities for the sample containing 16 mol% of sitosterol. As the successively recorded diffraction patterns of all the samples showed no change with time and since all the data were processed in the same way, a relative comparison of the d_L values appears to be significant. Similar increases in d_L were observed when either non-deuterated or labeled sterol was incorporated, i.e. for two completely independent measurements.

All these features are compatible with a positioning of the sterols in the hydrocarbon region of the bilayer with the hydroxyl group just at the edge of the polar region. When sterol molecules are intercalated the distance between polar groups increases and water molecules can interpenetrate these groups giving rise to a lower scattering density. In the hydrocarbon region the presence of sterols leads to an increase of the scattering density.

3.2. The labeled samples

Fig. 5 shows the profiles of the bilayers for sitosterol and stigmasterol with deuterium-labeled sterol and with unlabeled sterol, and the difference between them. Even though the data sets were obtained in different samples we do not observe a significant change in the lattice spacing of samples with the same composition.

For the sitosterol sample, the difference profile displays a large positive peak around the bilayer center. The label profile was fitted with two Gaussian peaks using Eq. (5). The deuterium atoms are located, relatively to the bilayer center, at $x_0 = \pm(1.6 \pm 0.2$ Å) and with a distribution width of $\nu = 2.5 \pm 0.5$ Å. These parameters are obtained with good accuracy, as proved by the calculations performed by Gordeliy et al. [27]. Five structure factors are sufficient for these calculations even if the accuracy is lower since the label is in the center of the hydrophobic area.

The stigmasterol difference profile is much broader with three peaks in the region ± 15 Å. This profile was fitted in two different ways, i.e. by assuming either two coexisting locations of the

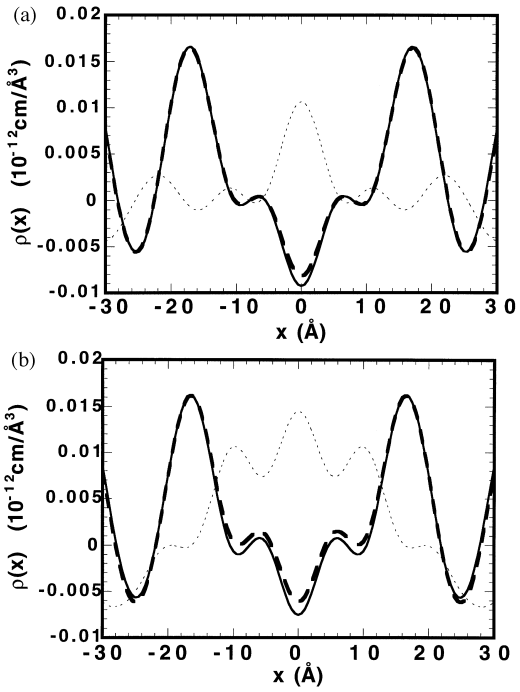

Fig. 5. Scattering profiles for the non-deuterated (dashed line) and the deuterated (solid line) samples, and difference Fourier profiles obtained by subtracting these profiles (dotted line). The difference profile has been multiplied by a factor of 10. (a) for the sitosterol 16 mol% sample; (b) for the stigmasterol 16 mol% sample.

label or only one. The calculation with two possible locations gave for the, $^2H_{25}$ atom, the locations $x_0 = \pm(2.3 \pm 0.2)$ Å and $x_0 = \pm(10 \pm 0.2)$ Å with the same width $\nu = (3.5 \pm 0.5)$ Å. The fitting with only one distribution gave $x_0 = \pm(6.1 \pm 0.3)$ Å and $\nu = (8.5 \pm 0.7)$ Å. For the stigmasterol, the presence of two possible positions next to each other, highly reduces the resolution of the measurement. The accuracy obtained for the parameters of the Gaussian (position, width, weight) strongly depends on the 'power' of the deuterium label [27] which is quite low in our case ($n = 0.16$).

The statistical precision in the values of x_0 and ν is quite high but does not include systematic errors such as those arising from the Lorentz correction, for example. These, however, will affect the results obtained from both samples in the same way.

4. Discussion and conclusions

In this paper we investigated the influence of two plant sterols, sitosterol and stigmasterol, in SPC membranes by neutron diffraction since previous studies had proved that the introduction of a double bond at position C_{22} of sitosterol, leading to stigmasterol, modifies the interaction of sterol with phospholipids by decreasing the sterol ordering effect on the surrounding lipid molecules [8,16].

SPC has the disadvantage for neutron scattering experiments to contain fatty acids with different chain lengths and a number of unsaturated bonds which induce a low degree of order in the macroscopic sample, preventing the measurement of high diffraction orders. We made the choice to continue our experiments with this phospholipid mixture since it is a good model for plant membranes [16] and it allows a more direct comparison with other experimental approaches. We observed only five orders for all our samples so the resolution of the profiles presented herein is rather low [28].

The first feature that can be compared is the hydrophobic thickness d_L of the bilayers. The values of d_L are directly measured from the density profile as the distance between the two maxima, therefore the low resolution of the experiment has a direct influence on its precision. Moreover, d_L may be influenced by the experimental conditions: temperature, hydration level, or lipid composition [5,23,25,29]. In the following we will not discuss the intrinsic values of d_L, but we will rather compare the effect of the two plant sterols on the hydrophobic thickness of SPC bilayers. This is possible first because we worked in such conditions that the experimental reproducibility for our profiles was of 0.1 Å and also because all experimental data were processed in the same way.

As described in Section 3.1, sitosterol and stigmasterol are embedded in the hydrocarbon region of the bilayer with their hydroxyl groups at the edge of the polar region; nevertheless, the two sterols have a different behavior: when stig-

masterol is incorporated at 16 mol%, its maximal solubility in SPC, no significant change of d_L is observed. On the other hand, sitosterol increases d_L by 1.2 Å when incorporated at the same concentration. The same results were obtained with 25-^{2}H sterols.

We have previously investigated the ability of sitosterol and stigmasterol to order the acyl chains of SPC by fluorescence polarization [16] and ^{2}H-NMR [8,9]. In the latter study we measured the segmental order parameters, Smol, for all the C–D bonds along the perdeuterated sn-2 acyl chain of DMPC incorporated as a molecular probe at a concentration of 10 mol% in SPC bilayers. The two sterols were able to increase all Smol when present at 16 mol%. Nevertheless, sitosterol was always more efficient than stigmasterol: at the plateau region (C_2–C_9) sitosterol increases the segmental order parameters by 23%, whereas stigmasterol increases them by only 10%; the difference being even higher when considering the chain positions near the bilayer center: +35% for sitosterol and +11% for stigmasterol.

These results suggest a correlation between plant sterol-inducing membrane ordering and an increase of the lipid core thickness. This is supported by a similar behavior of cholesterol, the major sterol in plasma membranes of mammalian cells (for review, see [1,2,4,30–32]). Indeed, when incorporated into liquid crystalline lipid bilayers, the membrane ordering induced by cholesterol (as detected by ^{2}H-NMR) is pictured as an increase in the hydrophobic bilayer thickness — as measured by X-ray or neutron diffraction [33–35]. The presence of cholesterol leads to a marked decrease of the number of gauche defects per chain which adopt preferentially *trans* conformations and then become longer (more stretched) [29,36]. By comparison, the same must occur when sitosterol is incorporated into SPC bilayers. However, the effect observed in our study is weaker: as seen in Table 4, even in the presence of 30 mol% of sitosterol, the increase of the hydrophobic thickness does not exceed 2 Å while 30 mol% of cholesterol leads to an increase of 3.9 Å when incorporated in the fluid phase of DMPC bilayers [35]. An explanation for this difference could be the composition of the bilayer itself: SPC contains a large amount of polyunsaturated fatty acids which are more mobile and difficult to order. Indeed, it has been shown that the condensing effect of cholesterol is weaker when phospholipids contain a large proportion of polyunsaturated fatty acid chains [16,37–39]; for example, its influence on segmental order parameters is twice as less in SPC than in DMPC bilayers [9]. One should also notice that cholesterol is always the most efficient molecule when compared with hydrocarbon chain ordering studies of precursors or derivatives of cholesterol [9,30,40]. For example, in the case of dioleyl PC the maximum stiffening effect of stigmastanol, the fully hydrogenated sitosterol, measured in terms of ^{2}H-NMR quadrupolar splitting, is only 50% that of cholesterol [40].

Our interest was also to investigate the molecular basis of the difference between sitosterol and stigmasterol. We synthesized both sterols deuterated at position 25 in the side chain and performed ^{2}H-NMR [10] and the present neutron diffraction studies. Location of the deuterated atom was possible as the difference between neutron diffraction profiles of bilayers containing non-labeled and labeled sterol gave access to the deuterium atoms spatial distribution (see Fig. 5), as described previously for different types of molecules by several authors [5,15,24,25]. The analysis of the difference profiles, ρ_{label}, obtained for sitosterol and stigmasterol revealed a different location for the deuterium atom of the two sterols. The deuterium atom of sitosterol is located, relative to the center, at ($\pm 1.6 \pm 0.2$) Å, suggesting that the side chain is stretched and mainly parallel to the adjacent fatty acid chains. This would allow numerous and efficient Van der Waals attractions to occur between sitosterol side chain and lipid chains and promote an efficient ordering effect near the center of the bilayer. This is in agreement with the high ordering effect of sitosterol in the center of the lipid bilayer shown by ^{2}H-NMR (see above). For stigmasterol the fitting gave access to two possible descriptions as discussed in Section 3.2: either an equilibrium between two well defined positions of the label, one at $x_0 = \pm 2.3$ Å, the other at $x_0 = \pm 10$ Å, or a broad distribution of location between 0 and

± 10 Å. From the ^{2}H-NMR work [10], where one single quadrupole splitting was observed in each case, these locations have to be in fast exchange on the microsecond time scale of ^{2}H-NMR. Since we cannot exclude that the undulations observed on the ρ_{label} profile are due to truncation effects and experimental errors on the structure factors, we cannot choose between these two models of stigmasterol side chain dynamics. In any case, the two are in favor of a delocalization of this side-chain in the lipid core.

In conclusion, the reported neutron diffraction experiments have demonstrated that the simple introduction of a Δ^{22} *trans* double bond in the lateral chain of sitosterol (leading to stigmasterol) is sufficient to totally differentiate the behavior. Compared to sitosterol, stigmasterol appears to have no significant effect on the hydrophobic thickness of SPC bilayers and to have a more delocalized side chain. Their different effect on the hydrophobic thickness may have a biological significance, as it may be a way to regulate some membrane functions. Indeed some proteins have their activity modulated by hydrophobic thickness changes induced by cholesterol [41,42]. Furthermore, it has been shown that sitosterol has the same properties as cholesterol (results presented herein and [8,16]) and so can be considered as a membrane reinforcer. On the contrary, stigmasterol has different effects: a limited ability to order acyl chains of SPC [8] and no effect on water permeability of vesicles of the same composition [8]. Its membrane function must be different and a metabolic role should be considered as trace amounts of this sterol have been reported to promote plant cell growth [43,44]. Finally, the different behavior of the two lateral chains of plant sterol provides a first explanation of the different activity of the two molecules: the neutron diffraction data presented herein demonstrate that the sitosterol side chain has a reduced conformational mobility, being mainly extended in the bilayer (to account for a localization of the 25-hydrogen at ± 1.6 Å) and may thus have optimum Van der Waals interactions with the surrounding lipids. Concerning stigmasterol, on the contrary, our results demonstrate a high mobility of its side chain although we cannot be more specific about the sort of movement involved.

Acknowledgements

We would like to thank warmly those who helped us, S. Wood and the ILL staff for neutrons and environment, Dr V. Gordeliy for his helpful advice on data reduction and Karine Sultan who typed the final version of the manuscript.

References

[1] P.L. Yeagle, Biochim. Biophys. Acta 822 (1985) 267.
[2] F.T. Presti, Membrane Fluidity Biol. 4 (1985) 97.
[3] J. Seelig, Q. Rev. Biophys. 10 (1977) 353.
[4] J.H. Davis, in: L. Finegold (Ed.), Cholesterol in Membrane Models, CRC Press, Boca Raton, 1993, p. 67.
[5] D.L. Worcester, N.P. Francks, J. Mol. Biol. 100 (1976) 359.
[6] M.G. Taylor, T. Akiyama, I.C.P. Smith, Chem. Phys. Lipids 29 (1981) 327.
[7] E.J. Dufourc, E.J. Parish, S. Chitrakorn, I.C.P. Smith, Biochemistry 23 (1984) 6062.
[8] I. Schuler, A. Milon, Y. Nakatani, G. Ourisson, A.M. Albrecht, P. Benveniste, M.A. Hartmann, Proc. Natl. Acad. Sci. U.S.A. 88 (1991) 6926.
[9] M.A. Krajewski-Bertrand, A. Milon, M.A. Hartmann, Chem. Phys. Lipids 63 (1992) 235.
[10] M.P. Marsan, W. Warnock, I. Muller, Y. Nakatani, G. Ourisson, A. Milon, J. Org. Chem. 61 (1996) 4252.
[11] G. Büldt, H.U. Gally, J. Seelig, G. Zaccai, J. Mol. Biol. 134 (1979) 673.
[12] G. Zaccai, G. Büldt, A. Seelig, J. Seelig, J. Mol. Biol. 134 (1979) 693.
[13] D.L. Worcester, in: D. Chapman, D.F.H. Wallach (Eds.), Biological Membranes, vol. 3, Academic Press, London, 1976, p. 153.
[14] G. Büldt, H.U. Gally, A. Seelig, J. Seelig, G. Zaccai, Nature 271 (1978) 182.
[15] E. Pebay-Peroula, E.J. Dufourc, A.G. Szabo, Biophys. Chem. 53 (1994) 45.
[16] I. Schuler, G. Duportail, N. Glasser, P. Benveniste, M.A. Hartmann, Biophys. Acta 1028 (1990) 82.
[17] A.M. Saxena, B.P. Schoenborn, Acta Cryst. A33 (1977) 813.
[18] A. Tardieu, V. Luzzati, J. Mol. Biol. 75 (1973) 711.
[19] J.F. Nagle, R. Zhang, S. Tristram-Nagle, W. Sun, H.I. Petrache, R.M. Suter, Biophys. J. 70 (1996) 1419.
[20] S.H. White, R.E. Jacobs, G.I. King, Biophys. J. 52 (1987) 663.
[21] The Merck Index, 1989, Merck and Co., Inc.
[22] G. Zaccai, J.K. Blasie, B.P. Schoenborn, Proc. Natl. Acad. Sci. U.S.A. 72 (1975) 376.

[23] G.E. King, S.H. White, Biophys. J. 49 (1986) 1047.
[24] P. Martel, A. Makriyannis, T. Mavromoustakos, K. Kelly, K.R. Jeffrey, Biochim. Biophys. Acta 1151 (1993) 51.
[25] K.C. Duff, A.J. Cudmore, J.P. Bradshaw, Biochim. Biophys. Acta 1145 (1993) 149.
[26] A. Léonard, Thèse de Doctorat de l'Université de Bordeaux I, Bordeaux, France, 1993.
[27] V.I. Gordeliy, N.I. Chernov, Acta Cryst. D53 (1997) 377.
[28] Y. Wu, K. He, S.J. Ludtke, H.W. Huang, Biophys. J. 68 (1995) 2361.
[29] J.P. Douliez, A. Léonard, E.J. Dufourc, J. Phys. Chem. 100 (1996) 18450.
[30] K.E. Bloch, CRC Crit. Rev. Biochem. 14 (1983) 47.
[31] M.R. Vist, J.H. Davis, Biochemistry 29 (1990) 451.
[32] M. Bloom, E. Evans, O.G. Mouritsen, Q. Rev. Biophys. 24 (1991) 293.
[33] G.W. Stockton, I.C. Smith, Chem. Phys. Lipids 17 (1976) 251.
[34] J.H. Ipsen, O.G. Mouritsen, M. Bloom, Biophys. J. 57 (1990) 405.
[35] A. Léonard, E.J. Dufourc, Biochimie 73 (1991) 1295.
[36] J.P. Douliez, A. Léonard, E.J. Dufourc, Biophys. J. 68 (1995) 1727.
[37] R.A. Demel, B. De Kruyff, Biochim. Biophys. Acta 457 (1976) 109.
[38] A. Kusumi, W.K. Subczinski, M. Pasenkiewicz-Gierula, J.S. Hyde, H. Merkle, Biophys. Biochim. Acta 854 (1986) 307.
[39] W.J. van Blitterswijk, B. Wieb van der Meer, H. Hilkmann, Biochemistry 26 (1987) 1746.
[40] R.K.G. Habiger, J.M. Cassal, H.J.M. Kempen, J. Seelig, Biochim. Biophys. Acta 1103 (1992) 69.
[41] O.G. Mouritsen, M. Bloom, Biophys. J. 46 (1984) 141.
[42] O.G. Mouritsen, in: D. Baeriswyl, M. Droz, A. Malaspinas, P. Martinoli (Eds.), Physics in Living Matter. Springer-Verlag, New York, 1986, p. 76.
[43] K. Grossmann, E.W. Weiler, J. Jung, Planta 164 (1985) 370.
[44] P.A. Haughan, J.R. Lenton, L.J. Goad, Phytochemistry 27 (1988) 2491.